Journal of Robotics, Networking and Artificial Life
Vol. 7(1); June (2020), pp. 63–67
DOI: https://doi.org/10.2991/jrnal.k.200512.013; ISSN 2405-9021; eISSN 2352-6386
https://www.atlantis-press.com/journals/jrnal

Research Article

Neuromorphic Computing in Autoassociative Memory with a Regular Spiking Neuron Model

Naruaki Takano[1,*], Takashi Kohno[2]

[1]Graduate School of Information Science and Technology, The University of Tokyo, 7-3-1 Hongo, Bunkyo-ku, Hongo, Bunkyo-ku, Tokyo 113-8656, Japan
[2]Institute of Industrial Science, The University of Tokyo, 4-6-1, Komaba, Meguro-ku, Tokyo 153-8505, Japan

ARTICLE INFO

Article History
Received 06 November 2019
Accepted 16 March 2020

Keywords
Spiking neural network
associative memory
DSSN model
spike frequency adaptation

ABSTRACT

Digital Spiking Silicon Neuron (DSSN) model is a qualitative neuron model specifically designed for efficient digital circuit implementation which exhibits high biological plausibility. In this study we analyzed the behavior of an autoassociative memory composed of 3-variable DSSN model which has a slow negative feedback variable that models the effect of slow ionic currents responsible for Spike Frequency Adaptation (SFA). We observed the network dynamics by altering the strength of SFA which is known to be dependent on Acetylcholine volume, together with the magnitude of neuronal interaction. By altering these parameters, we obtained various pattern retrieval dynamics, such as chaotic transitions within stored patterns or stable and high retrieval performance. In the end, we discuss potential applications of the obtained results for neuromorphic computing.

1. INTRODUCTION

Neuromorphic computing is an attempt to realize a computing architecture capable of complex and robust calculations with low power consumption, which is designed by either imitating or inspired by the information processing mechanisms in the nervous system.

Unlike the conventional von Neumann computer architecture in which CPU and memory units exist separately, the neuromorphic hardware generally has highly distributed computation and memory units. Such a massively parallelized computation which overcomes the von Neumann bottleneck is expected to reduce overall energy consumption.

Silicon Neuronal Networks (SiNNs) are a neuromorphic hardware that attempt to reproduce the electrophysiological activities in the nervous system by electronic circuits. Models of neurons, synaptic activities and designs of underlying algorithms are crucial factors as the components in the SiNNs. Many neuron models have been proposed for reproducing various traits of neurons. However, they generally undergo the problem of trade-off between implementation cost and biological plausibility [1].

Digital Spiking Silicon Neuron (DSSN) model is a qualitative neuron model which reproduces dynamical structure in various neuronal firing activities and is designed to be implemented efficiently on digital circuit [2].

As a fundamental model of neuromorphic computation, an all-to-all connected network composed of DSSN model has been implemented and autoassociative task was performed [3]. The network retrieved a stored pattern given corresponding corrupted input patterns, and its performance varied greatly on each neuron's parameters. It was shown that the performance is dependent on the class of the neuron model (Class 1 and 2 in Hodgkin's Classification).

In our study we adopt the equivalent system, however, we incorporate Regular Spiking class for each neuron. Regular Spiking class exhibit Spike Frequency Adaptation (SFA) which is a convergence of firing frequency from high value to a low value given a step current with sufficiently large magnitude.

Moreover, the strength of SFA is known to be reduced by cholinergic modulation [4] and it has been modeled on network of Hodgkin Huxley type neuron model [5,6]. We aim to apply and utilize the modulatory effect for neuromorphic computing. For this purpose, we studied network dynamics by altering corresponding parameters of the DSSN model.

2. NEURON AND SYNAPSE MODEL

Two variables in the DSSN model, membrane potential v and a variable n that represents a group of ion channels, are responsible for generating neuronal spikes.

Spike frequency adaptation is reproduced by introducing an additional slow negative feedback variable q, which results to 3-variable DSSN model [7]. For simplicity, we adopt the following 3-variable DSSN model with linear q-nullcline [7] instead of the nonlinear q-nullcline model [8].

*Corresponding author. Email: naruakitakano@sat.t.u-tokyo.ac.jp

$$\begin{aligned}\frac{dv}{dt} &= \frac{\phi}{\tau}\left(f(v) - n - q + I_0 + I_{\text{stim}}\right),\\ \frac{dn}{dt} &= \frac{1}{\tau}(g(v) - n),\\ \frac{dq}{dt} &= \frac{\varepsilon}{\tau}(v - v_0 - \alpha q),\end{aligned} \tag{1}$$

where,

$$f(v) = \begin{cases} a_{fn}(v - b_{fn})^2 + c_{fn} & (v < 0)\\ a_{fp}(v - b_{fp})^2 + c_{fp} & (v \geq 0),\end{cases} \tag{2}$$

$$g(v) = \begin{cases} a_{gn}(v - b_{gn})^2 + c_{gn} & (v < v_g)\\ a_{gp}(v - b_{gp})^2 + c_{gp} & (v \geq v_g).\end{cases} \tag{3}$$

Parameters a_{fn}, b_{fn}, c_{fn}, a_{fp}, b_{fp}, c_{fp} are tuned to reproduce the v nullcline. Similarly, parameters a_{gn}, b_{gn}, c_{gn}, a_{gp}, b_{gp}, c_{gp} determine the shape of the n nullcline. Parameter I_0 is a constant that model bias current and I_{stim} represents input stimulus. Since DSSN model is a qualitative model, all variables are dimensionless except t which is modeled such that its value is set approximately at a timescale of seconds. Parameters ϕ, τ and ε control time constants of variables v, n and q. In particular, ε controls decay time of adaptation dynamics.

Parameter α controls strength of SFA, which is defined as the difference of Inter-spike-Interval (ISI) between the initial and the converged state. When α is low, the effect of SFA is strong (see Figure 1). Since SFA is known to be reduced during cholinergic modulation, magnitude of α can be mapped to concentration of Acetylcholine during modulation.

Synaptic current of each neuron is modeled as,

$$\frac{dI_s}{dt} = \begin{cases} \alpha_{\text{syn}}(1 - I_s) & (v > 0)\\ -\beta_{\text{syn}} I_s & (v \leq 0),\end{cases} \tag{4}$$

where $\alpha_{\text{syn}} = 83.3$ and $\beta_{\text{syn}} = 333.3$.

3. NETWORK CONFIGURATION AND METHOD

Our network model is an all-to-all connected network of 256 neurons (3-variable DSSN model), and synaptic efficacy in each synapse is given by synaptic weight matrix W. External input to ith neuron is given as,

$$I^i_{\text{stim}} = c\sum_{j=1}^{N} W_{i,j} I^j_s + I^i_{\text{ext}}, \tag{5}$$

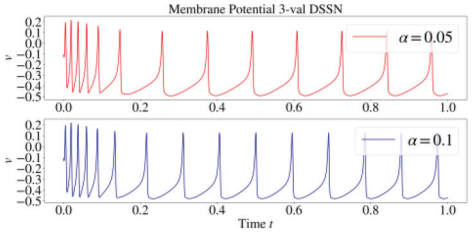

Figure 1 | Spike frequency adaptation observed in DSSN model for α = 0.05 (Top) and 0.1 (Bottom).

where c is a parameter that denotes the magnitude of neuronal interaction and I_{ext} is a constant bias current.

Four mutually orthogonal patterns (Figure 2a) were stored in the network by configuring synaptic weight matrix W by the following correlation rule,

$$W_{i,j} = \begin{cases} \frac{1}{p}\sum_{u=1}^{p} w_u x^u_i x^u_j & (i \neq j)\\ 0 & (i = j)\end{cases} \tag{6}$$
$$(p = 4, 1 \leq i,\ j \leq 256).$$

Here, x is a vector of size 256, where pixels in a pattern (16 × 16 pixels) are binary coded: +1 for black pixel and −1 for white pixel. w_u encodes weight bias of each pattern which are set as $w_u = 1.0$ (u = 1, 2, 3, 4) in the following simulations unless explicitly noted. Based on the stored patterns, we produced sets of corrupted input patterns, where certain percentage of randomly selected pixels are inverted. Figure 2b shows an example of sets of input data computed based on Pattern 1.

The autoassociative task is performed as follows: First, we initialized the network state with corrupted input data by injecting step current I_{ext} = 0.15 for 0.5 s (1334 timesteps) to the neurons that encode black pixel. Then, we stimulated all the neurons with I_{ext} = 0.15 to evoke repetitive neuronal activity.

We evaluated the network state by introducing Phase Synchronization Index (PSI) which quantifies the level of synchronization, and an overlap index M_u which quantifies the similarity between firing times of every neuron and uth stored pattern. Based on the firing phase in the repetitive firing activity, PSI and overlap between the network output is computed by,

$$\text{PSI}(t) = \frac{1}{N}\left|\sum_{j=1}^{N} \exp(i\phi_j(t))\right|, \tag{7}$$

and

$$M_u(t) = \frac{1}{N}\left|\sum_{j=1}^{N} x^u_j \exp(i\phi_j(t))\right|, \tag{8}$$

(i: imaginary number)

where firing phase of neuron j is defined as,

$$\phi_j(t) = 2\pi k + 2\pi\frac{t - t^k_j}{t^{k+1}_j - t^k_j}. \tag{9}$$

(t^k:k^{th} firing time of neuron j)

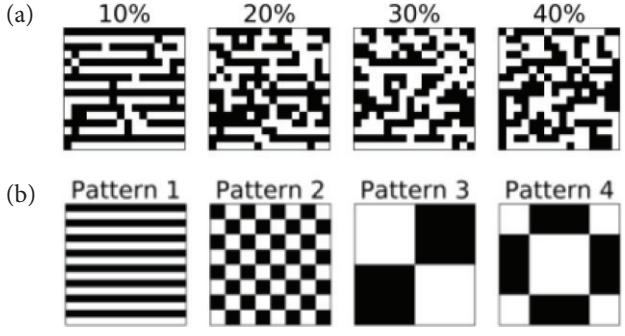

Figure 2 | (a) Stored patterns. (b) Input data (based on Pattern 1).

4. SIMULATION RESULTS

4.1. Weak Neuronal Interaction

We obtained stable overlap dynamics and high retrieval performance at the weak neuronal interaction region (c = 0.005). Figure 3 shows a successful retrieval process of Pattern 1. Figure 4 shows the retrieval performance evaluated over 100 trials for each value of α. Each trial was performed until t = 10. For α = 0.05 and 0.1, the successful retrieval rate keeps higher than 90% when the error rate is equal to 30% or less, which is comparable with network of class 2 neurons [3].

The superiority of retrieval performance can be reasoned by biphasic (Type 2) Phase Response Curve (PRC) [9] of neurons (Figure 5). It is known that slow negative feedback current is responsible for Type 2 PRC [5]. In addition, it is commonly known that most class 2 neurons have Type 2 PRC. These results support the comparable performance between network of class 2 neurons and our model.

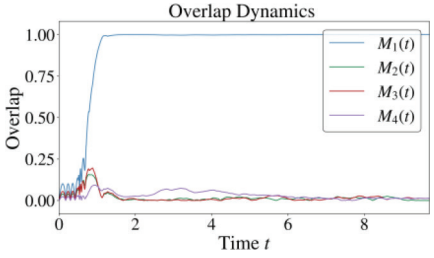

Figure 3 | Overlap dynamics in a successful retrieval process.

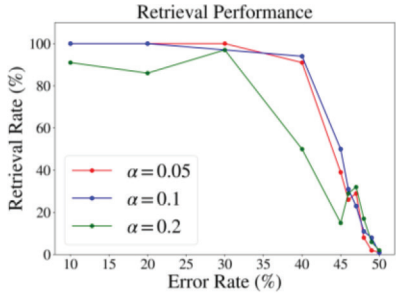

Figure 4 | Retrieval performance. x-axis shows error rate of the input pattern. y-axis is the percentage of successful retrieval. Successful retrieval was defined when PSI and overlap of corresponding input pattern exceeded 0.9.

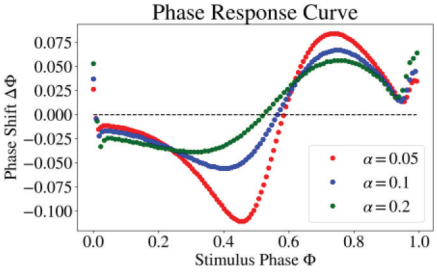

Figure 5 | Phase response curve of 3-variable DSSN model.

Phase response curve of Regular Spiking class neuron was computed by applying a perturbation only after the adaptation has fully stabilized to determine a unique firing period. As a result, we found that the zero-phase-shift-crossing point is essentially altered by α which in effect alters the overall retrieval performance. In other words, we may be able to design optimal PRC with α for retrieval tasks.

Magnitude of phase shift ($\Delta\Phi$) may not be an essential factor of the performance since increasing the magnitude of neuronal interaction did not give significant improvements (Figure 6).

4.2. Moderate Neuronal Interaction

We observed chaotic transition within stored patterns (Chaotic itineracy) when we set moderate neuronal interaction (c = 0.05). Figure 7a shows overlap dynamics with different α. Figure 7b is the staying period distribution without distinguishing patterns which were retrieved for a certain time. Maximum staying period was extended by decreasing α.

Previous study with the discrete Hopfield Network showed that adaptation term has a similar effect as a temperature term which is

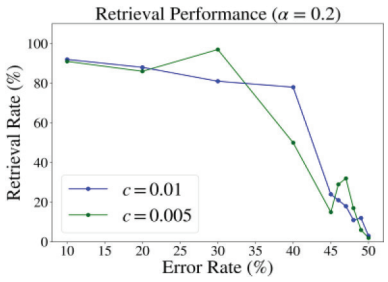

Figure 6 | Retrieval performance at c = 0.005 and 0.01 (α = 0.2).

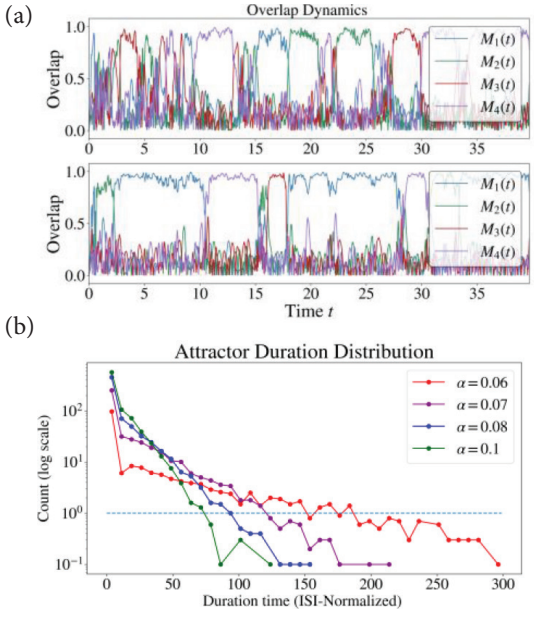

Figure 7 | (a) Overlap for c = 0.05. (Top) α = 0.1, (Bottom): α = 0.07. (b) Duration distribution (ISI-Normalized) of the pattern retrieval. Averaged from 10 trials of t = 1000 simulation and 40 bins. Retrieval is defined when overlap exceeded 0.8. Dashed blue line shows when count = 1.0.

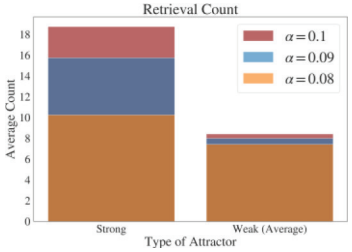

Figure 8 | Retrieval count of strong attractor and average count of weak attractors. Average computed from 40 trials.

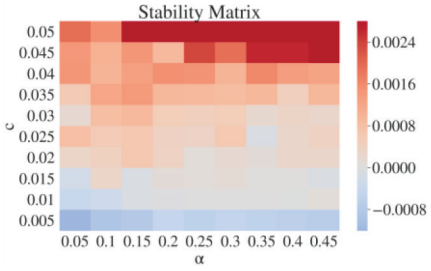

Figure 9 | Stability matrix computed from gradient of average divergence (log scale) between fiducial trajectories and 10 perturbed trajectories for each fiducial trajectory. Color bar shows gradient value.

known to destabilize attractors [6]. Similarly, in our model, variable q and SFA strength α is assumed to be responsible for destabilization of attractors leading to chaotic itineracy.

We then introduced heterogeneity in the network by grading each stored pattern with weight bias w_u. "Strong attractors" and "weak attractors" were distinguished by the size of w_u. We set $w_1 = 1.03$ and $w_{2,3,4} = 1.0$ (Pattern 1 corresponds to the strong attractor and the others weak). Then, we counted how often each pattern was retrieved (when overlap for the pattern exceeded 0.8) and observed the preference of attractor strength being modulated by α (Figure 8). Strong preference for strong attractor is observed at $\alpha = 0.1$, whereas the preference is relaxed as α is decreased.

4.3. Transition of Dynamical Behavior

Effects of c and α on the network's dynamical behavior is analyzed in the following stability matrix (Figure 9). Each value of the matrix is computed by calculating the gradient of the log-scaled Euclidean distance between fiducial trajectories (vector of v, n, q, I_s of 256 neurons) and perturbed trajectories. The value approximates largest Lyapunov exponent of 1024 dimension dynamical system. We confirmed that the system is stable at small c region (the gradient of divergence is 0 or below), and becomes chaotic at larger c (positive gradient of divergence). Stability may also be altered by α where smaller value leads to more stable dynamics, although further detailed analysis is needed.

5. DISCUSSION

We constructed an autoassociative memory composed of 3-variable DSSN model which exhibit SFA. As a result, various dynamics were observed at different parameter regions of c and α. By setting small c value, the effect of neuronal interaction may be considered as perturbations applied to each neuron, therefore evoking a characteristic of PRC: Type 2 PRC caused from the slow feedback current led to high retrieval performance. On the other hand, the synchronous network behavior switches to chaotic itineracy when c is increased. In this region, it can be assumed that destabilization effect caused by SFA [6] becomes more significant.

To model the level of Acetylcholine volume, we then investigated α-dependent effects at the above distinct regions resulting in rich dynamics. Although some biological correspondence, especially on the modulation of attractor strength preference (Figure 8) is discussed in the prior research [6], biological plausibility of our numerical simulation results such as duration distribution of the retrieval (Figure 7) need to be discussed in future.

From the engineering perspective, it is known that all-to-all connected networks are applicable to solving optimization problems [10]. Moreover, chaotic dynamics can be utilized to escape the local minima and obtain the global minima [11]. Similarly, our spiking neural network may be developed to solve optimization problems on low power hardware in the future. All results in this work were obtained by floating-point operations on software simulation (Euler method $dt = 0.000375$). One of the future works is to implement our models in fixed-point operations on FPGA devices.

APPENDIX

Table 1 | Parameter set for 3-variable DSSN model

Par.	Val.	Par.	Val.	Par.	Val.
a_{fn}	8.0	b_{fn}	−0.25	c_{fn}	−0.5
a_{fp}	−8.0	b_{fp}	0.25	c_{fp}	0.5
a_{gn}	4.0	b_{gn}	$-2^{-4} - 2^{-5}$	c_{gn}	−0.77083333
a_{gp}	16.0	b_{gp}	$2^{-5} - 2^{-2}$	c_{gp}	−0.6875
τ	2^{-9}	ϕ	0.625	r_g	−0.26041666
ε	0.03	v_0	−0.41	I_0	−0.09

Par., Parameter; Val., Value. (v_0 and ε take original values in this paper.)

CONFLICTS OF INTEREST

The authors declare they have no conflicts of interest.

ACKNOWLEDGMENTS

This work was supported by JST SICORP Grant Number JPMJSC15H1, Japan.

REFERENCES

[1] E. M. Izhikevich, Which model to use for cortical spiking neurons?, IEEE Trans. Neural Netw. 15 (2004), 1063–1070.

[2] T. Kohno, K. Aihara, Digital spiking silicon neuron: concept and behaviors in GJ-coupled network, Proceedings of International Symposium on Artificial Life and Robotics, Beppu, 2007, pp. OS3–OS6.

[3] J. Li, Y. Katori, T. Kohno, An FPGA-based silicon neuronal network with selectable excitability silicon neurons, Front. Neurosci. 6 (2012), 183.
[4] A.C. Tang, A.M. Bartels, T.J. Sejnowski, Effects of cholinergic modulation on responses of neocortical neurons to fluctuating input, Cereb. Cortex 7 (1997), 502–509.
[5] J.P. Roach, E. Ben-Jacob, L.M. Sander, M.R. Zochowski, Formation and dynamics of waves in a cortical model of cholinergic modulation, PLoS Comput. Biol. 11 (2015), e1004449.
[6] J.P. Roach, L.M. Sander, M.R. Zochowski, Memory recall and spike-frequency adaptation, Phys. Rev. E 93 (2016), 052307.
[7] W. Kobayashi, T. Kohno, K. Aihara, 3-Variable digital spiking silicon neuron, Proceedings of the 24th Workshop on Circuit and Systems, Hyogo, 2011, pp. 1–5 (in Japanese).
[8] T. Nanami, T. Kohno, Simple cortical and thalamic neuron models for digital arithmetic circuit implementation, Front. Neurosci. 10 (2016), 181.
[9] B. Ermentrout, Type I membranes, phase resetting curves and synchrony, Neural Comput. 8 (1996), 979–1001.
[10] J.J. Hopfield, D.W. Tank, 'Neural' computation of decisions in optimization problems, Biol. Cybern. 52 (1985), 141–152.
[11] H. Nozawa, Solution of the optimization problem using the neural network model as a globally coupled map, Phys. D 75 (1994), 179–189.

AUTHORS INTRODUCTION

Mr. Naruaki Takano

He is a graduate student at the University of Tokyo, Graduate School of Information Science and Technology. He received his B.S. in Information Science from Tokyo Institute of Technology in 2018. His research interests include computational neuroscience and network modeling.

Dr. Takashi Kohno

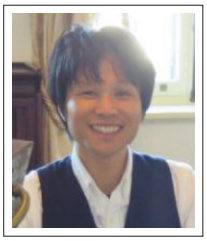

He has been with the Institute of Industrial Science at the University of Tokyo, Japan since 2006, where he is currently a Professor. He received the BE degree in medicine in 1996 and the PhD degree in mathematical engineering in 2002 from the University of Tokyo, Japan.